Glutamate 47 in 1-Aminocyclopropane-1-carboxylate Synthase Is a Major Specificity Determinant†

Darla L. McCarthy,‡,§ Guido Capitani,|| Liang Feng,‡,⊥ Markus G. Gruetter,|| and Jack F. Kirsch*,‡

Department of Molecular and Cell Biology, Division of Biochemistry and Molecular Biology, 229 Stanley Hall, University of California, Berkeley, California 94720-3206, and Biochemisches Institut der Universität Zürich, Winterthurerstrasse 190, CH-8057 Zürich, Switzerland

Received May 22, 2001; Revised Manuscript Received August 9, 2001

ABSTRACT: Glutamate 47 is conserved in 1-aminocyclopropane-1-carboxylate (ACC) synthases and is positioned near the sulfonium pole of (*S*,*S*)-*S*-adenosyl-L-methionine (SAM) in the modeled pyridoxal phosphate quinonoid complex with SAM. E47Q and E47D constructs of ACC synthase were made to investigate a putative ionic interaction between Glu47 and SAM. The k_{cat}/K_m values for the conversion of (*S*,*S*)-SAM to ACC and methylthioadenosine (MTA) are depressed 630- and 25-fold for the E47Q and E47D enzymes, respectively. The decreases in the specificity constants are due to reductions in k_{cat} for both mutant enzymes, and a 5-fold increase in K_m for the E47Q enzyme. Importantly, much smaller effects were observed for the kinetic parameters of reactions with the alternate substrates L-vinylglycine (L-VG) (deamination to form α-ketobutyrate and ammonia) and L-alanine (transamination to form pyruvate), which have uncharged side chains. L-VG is both a substrate and a mechanism-based inactivator of the enzyme [Feng, L., and Kirsch, J. F. (2000) *Biochemistry 39*, 2436−2444], but the partition ratio, k_{cat}/k_{inact}, is unaffected by the Glu47 mutations. ACC synthase primarily catalyzes the β,γ-elimination of MTA from the (*R*,*S*) diastereomer of SAM to produce L-VG [Satoh, S., and Yang, S. F. (1989) *Arch. Biochem. Biophys. 271*, 107−112], but catalyzes the formation of ACC to a lesser extent via α,γ-elimination of MTA. The partition ratios for ($\alpha,\gamma/\beta,\gamma$)-elimination on (*R*,*S*)-SAM are 0.4, ≤0.014, and ≤0.08 for the wild-type, E47Q, and E47D enzymes, respectively. The results of these experiments strongly support a role for Glu47 as an anchor for the sulfonium pole of (*S*,*S*)-SAM, and consequently a role as an active site determinant of reaction specificity.

The plant hormone ethylene is responsible for regulating many aspects of plant growth, development, and senescence (*1*). Formation of the biosynthetic precursor of ethylene, 1-aminocyclopropane-1-carboxylate (ACC),[1] is catalyzed by ACC synthase (*S*-adenosyl-L-methionine methylthioadenosine lyase, EC 4.4.1.14), a pyridoxal phosphate (PLP)-dependent enzyme. ACC synthase effects the α,γ-elimination of methylthioadenosine (MTA) from *S*-adenosyl-L-methionine (SAM) to produce ACC, as shown in reaction 1 of Chart 1. The conversion of SAM to ACC is the committed and rate-determining step in ethylene biosynthesis (*1*). Therefore, the mechanisms of catalysis by, and inhibition of, ACC synthase are additionally of great agricultural interest.

The ACC synthase catalytic mechanism has been characterized by site-directed mutagenesis and kinetic and spectroscopic investigations (*2*, *3*). The proposed mechanism for formation of ACC by this enzyme is an α,γ-elimination of MTA from the external aldimine of SAM (Scheme 1) (*4*, *5*). ACC synthase catalyzes several secondary reactions, including β,γ-elimination of MTA from (*R*,*S*)-SAM to form vinylglycine (L-VG) (*6*, *7*), deamination of L-VG (*8*), and transamination of various L-amino acids (*9*). However, it is clear that ACC synthase has primarily evolved for its role in ethylene biosynthesis; the rate of catalysis of the α,γ-elimination from SAM is diffusion-controlled (*3*), unlike those of the secondary reactions.

The "stickiness" of SAM in binding to ACC synthase likely emanates in part from specific interactions of the sulfonium ion with the enzyme. Our molecular model of (*S*,*S*)-SAM in the active site of ACC synthase is compatible with the hypothesis that Glu47 interacts with the sulfonium pole. We report here the results of an investigation into the role of Glu47 in binding and catalysis of the reactions of SAM and other substrates of ACC synthase.

† This work was supported by USDA Grant 98-35304-6743 to D.L.M., by NIH Grant GM35393 to J.F.K., and by the Baugarten Foundation, Zürich (support to M.G.G.).

* To whom correspondence should be addressed. Telephone: (510) 642-6368. Fax: (510) 642-6368. E-mail: jfkirsch@uclink4.berkeley.edu.

‡ University of California.

§ Present address: Department of Chemistry and Biochemistry, Calvin College, 3201 Burton St. SE, Grand Rapids, MI 49546.

|| Biochemisches Institut der Universität Zürich.

⊥ Present address: Department of Molecular Biophysics and Biochemistry, Yale University, New Haven, CT 06520.

[1] Abbreviations: ACC, 1-aminocyclopropane-1-carboxylate; AMA, [(2-aminooxy)ethyl](5′-deoxyadenosin-5′-yl)(methyl)sulfonium; AVG, aminoethoxyvinylglycine; α-KB, α-ketobutyrate; MTA, 5′-methylthioadenosine; NMR, nuclear magnetic resonance; PDB, Protein Data Bank; PIR, Protein Information Resource; PRF, Protein Research Foundation; PLP, pyridoxal 5′-phosphate; PMP, pyridoxamine 5′-phosphate; SAM, *S*-adenosyl-L-methionine; TAPS, 3-{[tris(hydroxymethyl)methyl]amino}-1-propanesulfonic acid; L-VG, L-vinylglycine; WT, wild-type.

10.1021/bi011050z CCC: $20.00
Published on Web 09/18/2001

Chart 1

Reaction 1. α, γ-elimination of MTA from (*S,S*) SAM

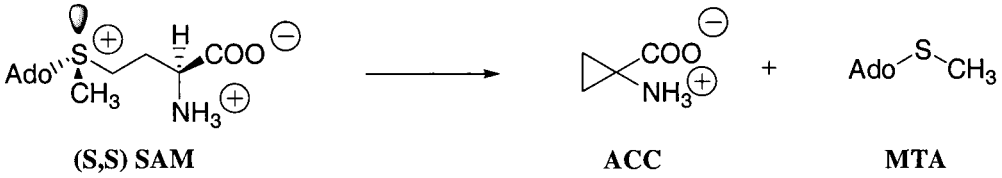

(S,S) SAM **ACC** **MTA**

Reaction 2. β, γ-elimination of MTA from (*R,S*) SAM

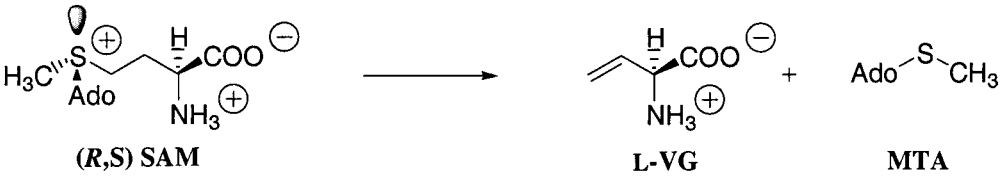

(*R*,S) SAM **L-VG** **MTA**

Reaction 3. Deamination of L-Vinylglycine/Inactivation

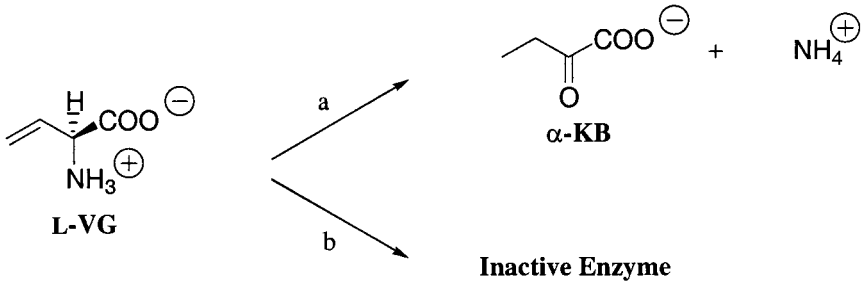

L-VG **α-KB** **Inactive Enzyme**

Reaction 4. Transamination of L-Amino Acids

Scheme 1: Proposed Mechanism for α,γ-Elimination of MTA from ACC Synthase (*4*, *5*)[a]

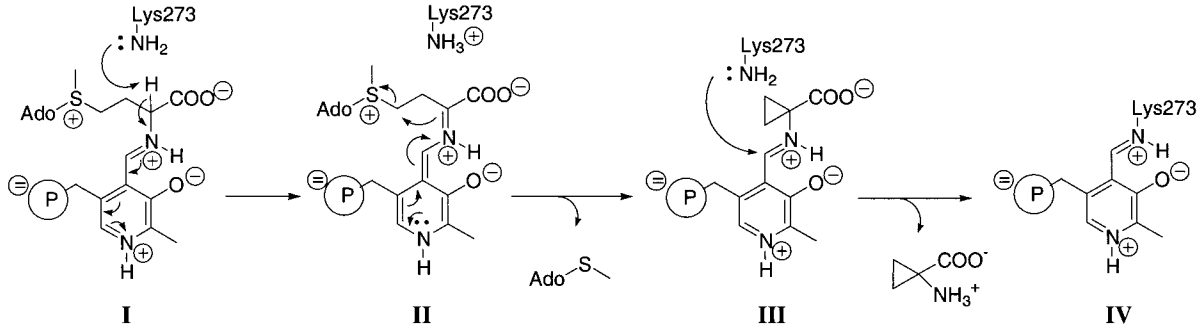

I **II** **III** **IV**

[a] The C_α proton is abstracted from the SAM−PLP external aldimine (**I**) by Lys273 to form a quinonoid species (**II**). Electrons are directed to C_γ, effecting the α,γ-elimination of MTA and formation of the ACC external aldimine (**III**), which undergoes transaldimination to release ACC and regenerate free enzyme (**IV**).

EXPERIMENTAL PROCEDURES

Materials. SAM [a mixture of the (*S,S*) and (*R,S*) diastereomers] was purchased from Calbiochem. L-VG, L-alanine, inorganic pyrophosphatase (I1643), and L-glutamate dehydrogenase (bovine liver, type VI, G2009) were obtained from Sigma. Other chemicals and biochemicals were of the highest quality commercially available.

Mutagenesis, Expression, and Purification of ACC Synthase. Mutagenesis was performed by recombinant PCR using oligonucleotides 5′-ATTATTCAGATGGGCTTAGCAGATAATCAGCTCTG-3′ and 5′-ATTATTCAGATGGGCTTAGCACAAAATCAGCTCTG-3′, and their complementary strands, for preparation of the E47D and E47Q constructs, respectively. Enzymes were expressed in, and purified from, *Escherichia coli* strain BL21(DE3)pLysS containing the expression vector pET19b with the apple ACC synthase gene for the wild type (WT), E47Q, or E47D, as previously described (*2*).

Modeling of (S,S)-SAM into the Active Site of ACC Synthase. An atomic model for (*S,S*)-SAM was retrieved from the HIC-UP server (*11*) and manually positioned into the active site of ACC synthase with the program O (*12*).

The crystallographic structure of ACC synthase complexed with the inhibitor 1-aminoethoxyvinylglycine (AVG) (G. Capitani et al., unpublished data) provided the template for the protein part of the model. The structure of the unliganded enzyme (*10*) was also considered in the modeling process. The interaction of the adenosyl moiety of (*S*,*S*)-SAM with the enzyme was modeled from preliminary crystallographic results (G. Capitani et al., unpublished data) at 2.0 Å resolution of a cocrystal of ACC synthase with an oxime-forming substrate analogue of (*S*,*S*)-SAM {[(2-aminooxy)-ethyl](5′-deoxyadenosin-5′-yl)(methyl)sulfonium (AMA)} (*13*). The model was energy-minimized with X-PLOR version 3.851, imposing harmonic restraints on the positions of water molecules. The energy minimization involved 300 cycles of Powell dynamics, with a linear distance-dependent dielectric function for electrostatic interactions. The parameter and topology files used for the minimization were PARAM19.PRO and TOPH19.PRO for the protein. For the SAM−PLP adduct, the topology and the parameter file were custom-made; for the adenosine moiety of the adduct, the custom files were based on the adenine entry of the standard PARAM11.DNA and TOPH11.DNA files.

Preparation of Enantiomerically Pure (S,S)-SAM. Enantiomerically pure (*S*,*S*)-SAM was enzymatically synthesized from ATP and methionine by SAM synthetase. This enzyme was expressed in *E. coli* strain DM22pK8 bearing the *metK* gene in pBR322, kindly provided by G. Markham (Fox Chase Cancer Institute, Philadelphia, PA). Cells were cultured and lysed, and the preparative-scale procedure for enzymatic synthesis of (*S*,*S*)-SAM described by Park et al. (*14*) was employed with a few modifications. First, 400 μL of freshly prepared crude cell lysate of DM22pK8 cells was added to 20 mL of a solution containing 100 mM Tris-HCl (pH 8.0), 50 mM KCl, 25 mM $MgCl_2$, 13 mM ATP, 1 mM EDTA, 8% β-mercaptoethanol, 10 mM methionine, and 0.1 mg of inorganic pyrophosphatase. The reaction mixture was incubated with gentle stirring on ice, with hourly additions of 400 μL aliquots of crude cell lysate. A final 400 μL of cell lysate and 0.1 mg of inorganic pyrophosphatase were added after 3 h, and the solution was incubated for an additional 1 h at 25 °C. The reaction was quenched by addition of HCl to 1 N and the mixture chilled on ice for 10 min. Precipitated protein was removed by centrifugation, and the supernatant was applied to a column containing Dowex 50W-8 (20−50 mesh) resin. After the column had been washed with 1 N HCl, (*S*,*S*)-SAM was eluted with 6 N HCl. (*S*,*S*)-SAM was recovered from the eluate by precipitation with Reinecke salt (*15*). The purity of the product was judged by NMR (*16*) to be >95% (*S*,*S*)-SAM. It was stored at −20 °C, and remained enantiomerically pure for more than 12 months.

Preparation of (R,S)-SAM. (*R*,*S*)-SAM was separated chromatographically from (*R*,*S*)-SAM-enriched mixtures of (*R*,*S*)- and (*S*,*S*)-SAM diastereomers that had been synthesized by methylation of *S*-adenosyl-L-homocysteine with iodomethane (*17*). The compounds were resolved by HPLC according to the method of Beaudouin et al. (*18*). A Nucleosil 100 C8 5 μm column (150 mm × 4.6 mm) was used with a 30 mm guard column containing the same silica resin. (*R*,*S*)-SAM was collected from the column, and rechromatographed to obtain a >95% pure sample. Column eluent containing (*R*,*S*)-SAM was lyophilized, resuspended in water, and stored at −20 °C. No detectable racemization, as judged by HPLC, was noted over a period of 4 months. Control experiments showed that the high concentration of salts from the HPLC elution buffer contaminating (*R*,*S*)-SAM stock solutions had no effect on catalysis by ACC synthase under the conditions used for the assays.

Kinetic Assays. α,γ- and β,γ-eliminations of MTA from (*S*,*S*)- and (*R*,*S*)-SAM, respectively, were monitored by a continuous assay that follows MTA production (*2*). The enantiomeric purities of the two SAM diastereomers were shown to be >95% by HPLC analysis (*18*) prior to the kinetic experiments. To prevent overestimation of the rates of reaction with (*R*,*S*)-SAM, only those rates following an initial "burst" due to elimination of MTA from residual (*S*,*S*)-SAM were recorded. The assay for deamination of L-VG was carried out with a continuous coupled assay utilizing glutamate dehydrogenase (*8*).

Transamination of L-alanine in single-turnover assays was monitored fluorimetrically. Accumulation of the PMP form of ACC synthase (0.6 μM) after addition of L-alanine was observed by following the emission of light at 390 nm upon excitation of the enzyme at 330 nm. The experiments were performed on a Perkin-Elmer LS50B luminescence spectrometer with an excitation slit width of 2.5 nm and an emission slit width of 8 nm.

Effects of Viscosity on the Kinetic Parameters for WT and E47D. Viscosity variation experiments were carried out as previously described for WT and Y233F ACC synthase (*3*), except that the buffers contained 5 μM PLP.

Spectrophotometric pK_a Determinations. The pK_as of the internal aldimines of E47Q and E47D ACC synthase were determined as described previously (*3*) using 12.3 and 11.4 μM solutions of the enzymes, respectively.

Determination of Reaction Partition Ratios. The partition ratios, k_{cat}/k_{inact}, for turnover and inactivation of the three ACC synthase enzymes by L-VG were determined as previously described (*8*), except that the buffer was 200 mM TAPS (pH 8.5) and contained 20% glycerol and 2 μM PLP. Enzymes (11.4 μM WT, 11.3 μM E47Q, or 15.0 μM E47D ACC synthase) were each incubated with 0, 0.23, 0.46, 0.92, 1.16, 2.32, and 4.62 mM L-VG. The final residual enzyme activities were determined after 6 h, when no further significant loss of activity was observed compared to controls containing no L-VG.

The partition ratios, $k_{\alpha,\gamma-elim}/k_{\beta,\gamma-elim}$, for elimination of MTA from (*S*,*S*)- and (*R*,*S*)-SAM were determined by measuring the distributions of products after prolonged incubation of the three ACC synthase enzymes with (*S*,*S*)- and (*R*,*S*)-SAM, respectively. Enzyme (2 μM WT and E47Q, or 4 μM E47D) was incubated with each of the SAM diastereomers (at 150 μM) in 200 mM TAPS (pH 8.5) containing 5 μM PLP. The reaction mixtures were incubated at room temperature (approximately 23 °C) for 2 h, conditions under which the SAM diastereomers do not epimerize significantly (*17*). An aliquot of each reaction mixture was removed, and the amino acids were derivatized with trinitrobenzene sulfonate (*19*). The products were quantitated by HPLC. Samples were injected onto a Microsorb MV C18 5 μm column (250 mm × 4.6 mm) equilibrated with 40% acetonitrile containing 0.1% acetic acid. The amino acid derivatives were eluted in the same solvent and detected by UV absorption at 346 nm. The retention times for the L-VG

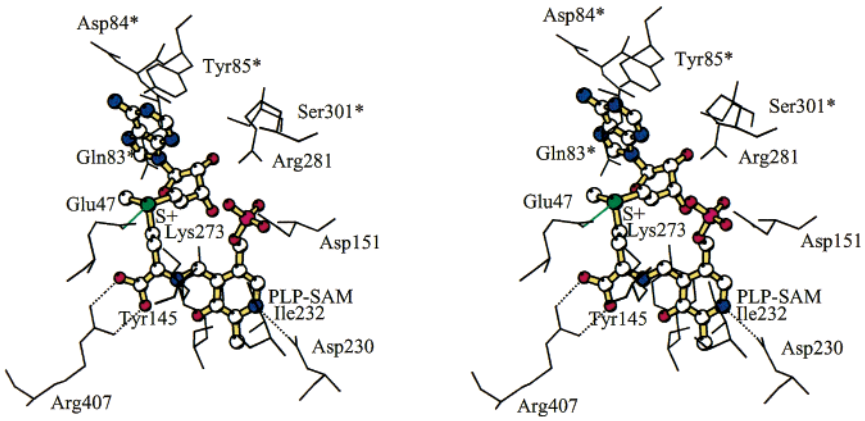

FIGURE 1: Active site view of the energy-minimized model for the quinonoid intermediate of the reaction of ACC synthase with (*S*,*S*)-SAM. Several important residues around the adduct, which is depicted in ball-and-stick mode, are represented in wire-frame mode. The atom color code is as follows: oxygen, red; nitrogen, blue; carbon, white; sulfur, green; and phosphorus, magenta. Some important hydrogen bonds are represented as dashed lines. A solid green line connects the S_γ atom of the adduct and the side chain carboxylate of Glu47 (distance of 4.5 Å). Asterisks denote the residues that belong to the neighboring subunit. Prepared with MOLSCRIPT (*32*).

and ACC derivatives were 7.2 and 8.9 min, respectively. A second aliquot of each reaction mixture was removed and analyzed for α-ketobutyrate (α-KB) by the spectrophotometric technique of Li and Kenyon (*20*). A third aliquot of each reaction mixture was analyzed for MTA by HPLC. Samples were injected onto a Nucleosil 100 C8 5 μm column (150 mm × 4.6 mm) equilibrated in solvent containing 40% methanol and 60% 0.1 M sodium acetate, 0.02 M citric acid, 0.93 mM octane sulfonate, and 0.12 mM EDTA (pH 4.6). MTA was eluted from the column in the same solvent with a retention time of 4.4 min, and was detected by UV absorption at 260 nm. The sums of the concentrations of ACC, L-VG, and α-KB formed in each reaction were similar to the respective concentrations of MTA formed. The reported $k_{\alpha,\gamma-\text{elim}}/k_{\beta,\gamma-\text{elim}}$ partition ratios were calculated as [ACC]/([L-VG] + [α-KB]) for each reaction mixture.

RESULTS

Modeling of SAM Bound to ACC Synthase (Quinonoid Intermediate). A tentative model of the (*S*,*S*)-SAM−PLP quinonoid intermediate was built (Figure 1) on the basis of the crystallographic structure of ACC synthase in complex with AVG, using additional information from the structure of the enzyme in complex with an oxime-forming analogue of SAM (AMA) and from the unliganded structure.

In the model, the SAM−PLP adduct is anchored to the protein through three main points.

(1) The adenine moiety of SAM stacks onto the phenol ring of Tyr85* (from the other subunit)[2] and interacts via its N6 amino group with Asp84*.

(2) The PLP moiety of the SAM−PLP adduct is bound to the protein through its phosphate group (salt bridge with Arg281 and hydrogen-bonding network of the phosphate with the neighboring residues). The PLP ring is also sandwiched between Tyr145 and Ile232. The pyridine nitrogen atom donates an electrostatically stabilized hydrogen bond to the side chain carboxylate of Asp230.

(3) The α-carboxylate moiety of the adduct makes a doubly hydrogen-bonded ion pair with the guanidino group of Arg407.

The energy-minimized model of the quinonoid intermediate displays reasonable geometry for the adduct and the protein−adduct interactions at all three anchoring points. Namely, the N−O distances in the doubly hydrogen-bonded ion pair are 2.7 and 2.8 Å, and the distance between the pyridine nitrogen of PLP and the nearest oxygen of Asp230 is 2.8 Å. The sulfonium pole in the model is found 4.5 Å from the nearest oxygen atom of Glu47. The side chain oxygen of Gln83* is 3.7 Å from the sulfur in the model.

Kinetic Parameters for Reactions Catalyzed by WT and E47 Mutant ACC Synthases. The four reactions effected by ACC synthase are shown in Chart 1. Reaction 1 is the physiological conversion of (*S*,*S*)-SAM to ACC and MTA. Reaction 2 is the β,γ-elimination of MTA from (*R*,*S*)-SAM, producing L-VG (*6*, *7*), which is also a substrate and an inactivator of ACC synthase (*8*). Reaction 3a is the deamination of L-VG to form α-KB and ammonia. L-VG is also a mechanism-based inhibitor of ACC synthase (reaction 3b), with a partition ratio, k_{cat}/k_{inact}, of 500. Reaction 4 is the transamination of various L-amino acids to form the corresponding α-ketoacids and the PMP form of ACC synthase (*9*).

The rate of reaction 1, and to a lesser extent that of reaction 2, would be expected to be particularly impacted by mutation of Glu47 if its side chain interacts with the sulfonium pole of (*S*,*S*)-SAM (see Discussion). In contrast, the rates of reactions 3 and 4, which occur with amino acids that lack cationic side chains, should suffer less. The steady-state kinetic parameters for reactions 1−4, listed in Table 1, substantiate the predicted role of the side chain of Glu47. The value of k_{cat}/K_m for reaction 1 is decreased 630- and 25-fold for the E47Q and E47D mutants, respectively. The effect is largely in k_{cat} (110-fold) rather than K_m (5-fold) for E47Q, and entirely in k_{cat} for E47D. The k_{cat}/K_m values for reaction 2 are less dramatically decreased in the E47Q and E47D mutant enzymes, with the specificity constant decreasing approximately 3-fold for each mutant enzyme. This effect is disbursed over both k_{cat} and K_m for E47Q, and rests entirely in k_{cat} for E47D.

[2] ACC synthase is a homodimeric protein. The two active sites in each homodimer lie near the subunit interfaces, with residues from each subunit contributing to the active site. Amino acid residues marked with asterisks are from the subunit that does not contribute the active site lysine (K273).

Table 1: Kinetic Parameters of Reactions Catalyzed by Wild-Type, E47Q, and E47D ACC Synthase[a]

	k_{cat} (s^{-1})	k_{cat}(WT)/k_{cat}(E47X)	K_m (mM)	K_m(WT)/K_m(E47X)	k_{cat}/K_m ($\times 10^{-3}$ M^{-1} s^{-1})	[k_{cat}/K_m(WT)]/[k_{cat}/K_m(E47X)]
Reaction 1: (*S*,*S*)-SAM → ACC + MTA						
WT	18 ± 2		0.026 ± 0.004		690 ± 130	
E47Q	0.16 ± 0.04	110 ± 30	0.14 ± 0.05	0.19 ± 0.07	1.1 ± 0.5	630 ± 300
E47D	0.69 ± 0.01	26 ± 3	0.025 ± 0.005	1.0 ± 0.3	28 ± 6	25 ± 7
Reaction 2: (*R*,*S*)-SAM → Vinylglycine + MTA						
WT[b]	0.079 ± 0.007		0.037 ± 0.007		2.1 ± 0.5	
E47Q	0.030 ± 0.003	2.6 ± 0.4	0.057 ± 0.019	0.65 ± 0.25	0.53 ± 0.18	4.0 ± 1.6
E47D	0.024 ± 0.001	3.3 ± 0.4	0.035 ± 0.015	1.1 ± 0.5	0.69 ± 0.30	3.0 ± 1.5
Reaction 3: L-Vinylglycine → α-Ketobutyrate + NH_4^+						
WT	0.71 ± 0.05		0.27 ± 0.05		2.6 ± 0.5	
E47Q	0.78 ± 0.05	0.91 ± 0.09	0.056 ± 0.010	4.8 ± 1.2	14 ± 2	0.19 ± 0.06
E47D	0.28 ± 0.03	2.5 ± 0.3	0.26 ± 0.04	1.0 ± 0.2	1.1 ± 0.2	2.4 ± 0.6
Reaction 4: E(PLP) + Alanine → E(PMP) + Pyruvate[c]						
WT	0.019 ± 0.001		37 ± 5		$(5.0 \pm 0.4) \times 10^{-7}$	
E47Q	0.026 ± 0.002	0.73 ± 0.07	19 ± 4	1.9 ± 0.5	$(1.4 \pm 0.2) \times 10^{-6}$	0.35 ± 0.06
E47D	0.022 ± 0.001	0.86 ± 0.06	17 ± 3	2.2 ± 0.5	$(1.3 \pm 0.2) \times 10^{-6}$	0.38 ± 0.07

[a] Reactions were monitored as described in Experimental Procedures. ACC synthase was incubated with various concentrations of substrates [9−350 μM (*S*,*S*)-SAM, 9−240 μM (*R*,*S*)-SAM, 0.014−1.14 mM L-VG, and 5−150 mM alanine] at 25 °C in 200 mM TAPS (pH 8.5) containing 1 μM PLP. The reported values are the average of at least two independent experiments for all but the deamination reactions. [b] The kinetic parameters reported for β,γ-elimination of MTA from (*R*,*S*)-SAM by the WT enzyme were obtained by multiplying the k_{cat} and k_{cat}/K_m values for formation of MTA from (*R*,*S*)-SAM by 0.72, the reciprocal of the quantity $1 + k_{\alpha,\gamma-elim}/k_{\beta,\gamma-elim}$. The partition ratio $k_{\alpha,\gamma-elim}/k_{\beta,\gamma-elim}$ was determined as described in Experimental Procedures. Because the E47Q and E47D mutants do not catalyze the α,γ-elimination of MTA from (*R*,*S*)-SAM at an appreciable rate, no adjustments were made to the observed rates of formation of MTA from (*R*,*S*)-SAM by those mutant enzymes. [c] Reported values were obtained from single-turnover assays at seven different alanine concentrations. Reaction conditions were as described above, except that the assay buffer contained 20% glycerol and no added PLP.

The Glu47 mutations result in much smaller effects on reactions 3 and 4. The E47Q mutation slightly *increases* the specificity of ACC synthase for both reactions 3 and 4. The 5-fold increase in k_{cat}/K_m for reaction 3 is due entirely to a decrease in K_m, and the 3-fold increase in k_{cat}/K_m for reaction 4 is due to minor effects on both k_{cat} and K_m. Similarly, a 3-fold increase in k_{cat}/K_m for reaction 4 catalyzed by E47D ACC synthase can be attributed to minor changes in both k_{cat} and K_m. The E47D mutation, however, results in a minor 2-fold decrease in k_{cat}/K_m for reaction 3, due to a decrease in k_{cat}.

Titration of the Internal Aldimine for WT, E47D, and E47Q. The kinetic parameters for catalysis of reactions 1−4 by ACC synthase are pH-dependent (ref *3* and unpublished results of D. L. McCarthy and A. C. Eliot). The pH profiles of k_{cat}/K_m are bell-shaped, with the pK_a of the ascending limb attributed to the pK_a of the α-amino group of the substrate, and the pK_a of the descending limb corresponding to the pK_a of the internal aldimine of ACC synthase. The pK_as of the internal aldimines of E47Q and E47D mutant ACC synthases were determined spectroscopically by monitoring the absorbancies of the protonated ($\lambda_{max} = 435$ nm) and unprotonated ($\lambda_{max} = 370$ nm) internal aldimine species as a function of pH. The averages of the pK_a values obtained at the two wavelengths for E47Q and E47D ACC synthases are 9.27 and 9.03, respectively. These values are sufficiently close to the WT pK_a value of 9.26 to rule out the possibility that the E47Q and E47D mutations significantly alter the pH profiles for reactions 1−4.

Effect of Viscosity on k_{cat}/K_m for E47D. The value of k_{cat}/K_m for the reaction of WT ACC synthase with (*S*,*S*)-SAM (6.90×10^5 M^{-1} s^{-1}) represents a diffusion-controlled reaction[3] (*3*). The k_{cat}/K_m for E47D ACC synthase (1.9×10^4 M^{-1} s^{-1}), however, is sufficiently reduced that it is unlikely to represent a fully diffusion-controlled reaction. Viscosity variation experiments were performed as previously described for WT and Y233F ACC synthase (*3*) to assess the extent to which diffusive processes contribute to k_{cat}/K_m for the mutant E47D enzyme. The dependence of the values of k_{cat}/K_m on macroscopic viscosity for the kinetic model of eq 1a is given in eq 1b (*21*), where η^o/η is the reciprocal of relative viscosity, η_{rel}, and k°_{-1} and k°_1 are the limiting rate constants when $\eta_{rel} = 1$. The values of k_{cat}/K_m recorded as a function of η^o/η and fitted to eq 1b yield the quantities k°_1, the rate constant for the association of enzyme with substrate, and k°_{-1}/k_2, the partition ratio (*P*) for the ES complex. The extent to which the reaction is diffusion-controlled is given by eq 1c.

$$E + S \underset{k_{-1}}{\overset{k_1}{\rightleftharpoons}} ES \xrightarrow{k_2} E + P \tag{1a}$$

$$k_{cat}/K_m = \frac{k^\circ_1(\eta^\circ/\eta)}{1 + (k^\circ_{-1}/k_2)(\eta^\circ/\eta)} \tag{1b}$$

$$\text{fraction diffusion-controlled} = \frac{k_2}{k^\circ_{-1} + k_2} = \frac{1}{1+P} \tag{1c}$$

$$\frac{(k_{cat}/K_m)^\circ}{k_{cat}/K_m} = \frac{P}{1+P} + \frac{1}{1+P}\eta_{rel} \tag{1d}$$

A comparative presentation of the effects of viscosity on the reactions catalyzed by WT and E47D ACC synthase is best achieved by a normalized linear plot according to eq 1d (*21*), where k_{cat}/K_m and $(k_{cat}/K_m)^\circ$ are the values of the

[3] The kinetic parameters provided herein for the α,γ-elimination of MTA from SAM ($k_{cat} = 18$ s^{-1}, $K_m = 26$ μM) differ from those published previously ($k_{cat} = 9$ s^{-1}, $K_m = 12$ μM) (*2*) in part because the present experiments employed enantiomerically pure (*S*,*S*)-SAM, whereas those reported previously were carried out with a commercially available mixture of SAM diastereomers [approximately 60% (*S*,*S*)-SAM and 40% (*R*,*S*)-SAM].

Scheme 2: Proposed Model for Partitioning of SAM between α,γ- and β,γ-Elimination To Form ACC and L-VG, Respectively (*7*), and for Partitioning of L-VG between Turnover and Inactivation (*8*)

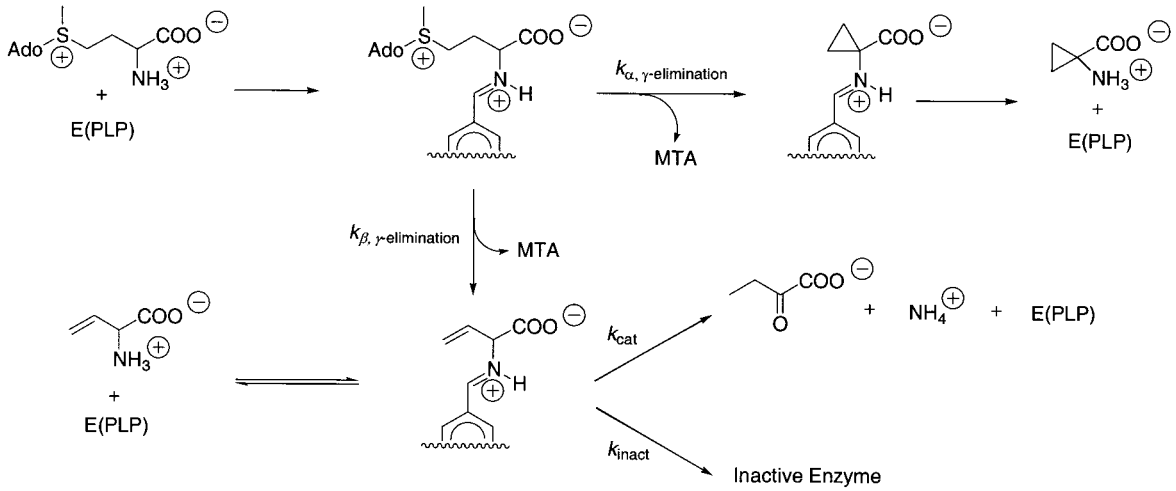

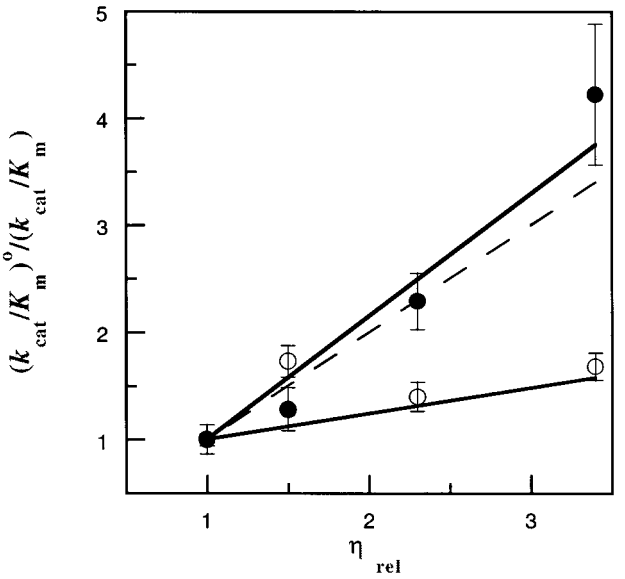

FIGURE 2: Plots of $(k_{cat}/K_m)°/(k_{cat}/K_m)$ vs η_{rel} for WT (●) and E47D ACC synthase (○) in buffer [50 mM TAPS (pH 8.4) and 5 μM PLP at 25 °C] containing 14, 24, or 32% sucrose. A theoretical fully diffusion-controlled reaction is represented by the dashed line having a slope of 1. The results shown here for WT ACC synthase agree closely with those obtained by Li et al. (*3*).

parameter in the presence or absence of viscosogen, respectively. The data are plotted accordingly in Figure 2, where the solid lines (i.e., fits to the data) were obtained from the partition ratios (*P*) extracted from nonlinear regression analysis on eq 1b (*21*). The slopes of the lines in Figure 2 are 1.15 and 0.24 for the WT and E47D enzymes, respectively. A completely diffusion-controlled rate of reaction should yield a slope of 1. The larger slope (1.15) obtained with WT ACC synthase is due to the fact that high concentrations of viscosogenic reagents cause additional solvent-dependent perturbations of the reaction parameters. The correction factors required to evaluate these nondiffusive effects of viscosogens may be obtained from evaluations of their effects on reactions of the enzyme that are not diffusion-controlled (*21*−*23*). Li et al. (*3*) employed Y233F ACC synthase, a mutant for which the rate of catalysis of α,γ-elimination of MTA from SAM is chemically controlled, for this purpose. Plots of $(k_{cat}/K_m)°/(k_{cat}/K_m)$ versus η_{rel} for the WT and Y233F enzymes yielded slopes of 1.20 and 0.22, respectively. The slopes of the lines in Figure 2 are nearly identical to those obtained by Li et al., and thus indicate that the rate of reaction of E47D ACC synthase with SAM is chemically controlled, as is the case for the corresponding reaction with Y233F ACC synthase.

Elimination and Inactivation Partition Ratios. Satoh and colleagues reported SAM-dependent inactivation of ACC synthase (*24*, *25*), and showed that the rate of inactivation is 3-fold greater for the (*R*,*S*) than for the (*S*,*S*) diastereomer (*7*). The likely mechanism for inactivation is shown in Scheme 2 where β,γ-elimination of MTA from SAM yields L-VG, which is both a substrate and an inactivator of ACC synthase (*8*). The postulated interaction of E47 with SAM suggests that the (α,γ)/(β,γ)-elimination ratio might be sensitive to the nature of the amino acid resident at position 47. Therefore, the (α,γ)/(β,γ)-elimination partition ratios for the three ACC synthase enzymes were determined with both (*S*,*S*)- and (*R*,*S*)-SAM. The inactivation partition ratio, k_{inact}/k_{cat}, for the reaction with L-VG for each enzyme was also determined.

The partition ratios for turnover and inactivation, k_{cat}/k_{inact}, by L-VG were determined to be 480 ± 20, 460 ± 10, and 110 ± 20 for the WT, E47Q, and E47D enzymes, respectively. The inactivation partition ratio is insensitive to the E47Q mutation, and the 4-fold decrease in k_{cat}/k_{inact} for the E47D enzyme can be largely attributed to the 2.5-fold decrease in k_{cat} for deamination of L-VG by that enzyme.

Incubation of the three ACC synthases with (*S*,*S*)-SAM did not result in accumulation of observable concentrations of the products of β,γ-elimination (α-KB, ammonia, and L-VG). A lower limit of 70 for the (α,γ)/(β,γ)-elimination partition ratios for these enzymes was estimated on the basis of a detection limit of 2 μM for α-KB and L-VG.

Although Glu47 does not significantly affect the (α,γ)/(β,γ)-elimination partition ratio with (*S*,*S*)-SAM, it does influence the (α,γ)/(β,γ)-elimination partition ratio when (*R*,*S*)-SAM is the substrate. The WT enzyme affords a partition ratio, $k_{\alpha,\gamma-elim}/k_{\beta,\gamma-elim}$, of 0.4 ± 0.1; i.e., approximately two in seven reactions at the active site of ACC synthase result in formation of ACC with (*R*,*S*)-SAM as the substrate. [Previous investigations of the reaction between ACC synthase and (*R*,*S*)-SAM suggested that the enzyme

could not catalyze the α,γ-elimination reaction with that substrate (*7*, *26*). This apparent discrepancy is due to the fact that the rate for α,γ-elimination of MTA from (*R*,*S*)-SAM is so low that ACC would not have been detected under the reaction and assay conditions used previously (*7*, *26*).] The E47Q and E47D mutant enzymes yield significantly lower $k_{\alpha,\gamma-\mathrm{elim}}/k_{\beta,\gamma-\mathrm{elim}}$ ratios (0.014 ± 0.004 and 0.08 ± 0.11,[4] respectively), confirming that Glu47 plays an important role in directing the reaction with (*R*,*S*)-SAM toward α,γ-elimination. The large partition ratios favoring α,γ-elimination of MTA from (*S*,*S*)-SAM, combined with the limited purity (>95%) of the (*R*,*S*)-SAM preparations, imply that the (*R*,*S*)-SAM elimination partition ratios measured for the mutant enzymes represent upper limits.

DISCUSSION

Model of SAM Bound to ACC Synthase. The model provides a three-dimensional framework for intermediate II of Scheme 1, which is the dominant resonance form of the carbanion at C_α (hybridized sp^2). The geometry of the carbanion in the present model is perfectly suited for the ensuing cyclization reaction because the C_γ and sulfur atoms are in line with the p_z-orbital of the C_α atom. The distance between the sulfonium pole and the nearest oxygen of Glu47 is ~4.5 Å in the model. Although this distance seemingly argues against the hypothesis of a strong electrostatic interaction, it must be recognized that the model is based on structures of ACC synthase complexes with substrate analogues that lack either the adenosine moiety (AVG) or the C_α and α-carboxylate group (AMA) of SAM (G. Capitani et al., unpublished results). The conformation of the protein in both cases is very similar to that observed in the unliganded enzyme (*10*), with the AVG-bound structure being slightly more closed than that of the unliganded enzyme. No large domain movement such as that seen in AATase (*27*) is observed. This movement is triggered in AATase by the interaction of the substrate with a residue of the small domain (Arg386) and another one from the large domain of the other subunit (Arg292*). This leads to a closure of the structure, with the small domain rotating by ~13° toward the large domain. The structural similarity between ACC synthase and AATase (*10*) raises the possibility that Arg407 on one side, and Tyr85* and other "helping" residues, including Asp84*, on the other side, may play an analogous role in triggering a closure of the enzyme when the natural substrate (*S*,*S*)-SAM associates. Even a modest degree of closure might serve to decrease the distance between the sulfonium pole and the carboxylate of Glu47 to as little as 3−3.5 Å. The fact that Glu47 is conserved in all 125 nonredundant ACC synthase sequences found in the GenBank, SwissProt, PDB, PIR, and PRF databases (searched September 12, 2000) is consistent with the prediction that Glu47 interacts with the sulfonium pole of SAM.

Another conserved residue that is modeled relatively near (3.7 Å) the sulfonium ion and may come closer upon closure of the enzyme is Gln83*. Interaction with the carboxamido oxygen atom may provide some additional electrostatic stabilization. Similar modeling with (*R*,*S*)-SAM results in the methyl group pointing toward Glu47 and Gln83*, thus shielding putative electrostatic interactions from the sulfonium pole, which would likely interfere with formation of the optimal geometry for α,γ-elimination.

Although the positively charged sulfonium ion provides an ideal site for binding interactions, few SAM-dependent enzymes employ this modality. A canonical SAM-binding motif that lacks residues that interact specifically with the sulfonium pole of SAM has been proposed on the basis of liganded structures and sequence analyses of several SAM-dependent methyltransferases (*28*, *29*). Only one SAM-dependent methyltransferase, glycine *N*-methyltransferase, is reported to harbor a negatively charged binding site residue (Glu15) that forms an ionic interaction with the sulfonium ion (*30*). One of the carboxylate oxygen atoms of Glu15 is 4.0 Å from the sulfonium pole of SAM in the liganded structure of glycine *N*-methyltransferase. It was additionally proposed to play a role in catalysis of the methyl transfer reaction. The apparent paucity of ion pair interactions with the sulfonium pole of SAM is not limited to methyltransferases. SAM decarboxylase is structurally dissimilar to these enzymes, and likewise does not appear to form an ionic interaction between the enzyme active site and the sulfonium pole of SAM (*31*).

The seemingly unusual interaction between the sulfonium pole of SAM and the strictly conserved Glu47 of ACC synthase is the subject of this investigation. Two mutants of ACC synthase, E47D and E47Q, were constructed to elucidate the role of Glu47 in binding of SAM and catalysis by ACC synthase. The E47D and E47Q variants respectively perturb the position of the carboxylate and the ionic charge itself.

Glu47 Plays Important Roles in Binding and Catalysis with the Substrate (S,S)-SAM. The kinetic parameters shown in Table 1 indicate that mutation of Glu47 in ACC synthase most significantly affects the α,γ-elimination of MTA from (*S*,*S*)-SAM. The specificity constant for ACC formation by the E47Q enzyme decreases 630-fold compared to that of the WT enzyme, due to both a decrease in k_{cat} (110-fold) and an increase in K_m (5-fold). The E47D enzyme also experiences a decrease in k_{cat}/K_m (25-fold), entirely attributable to a decrease in k_{cat}. On the other hand, the E47Q and E47D mutations of ACC synthase have only minor affects on the kinetic parameters of other reactions catalyzed by the enzyme. The k_{cat}, K_m, and k_{cat}/K_m parameters for each mutant are perturbed less than 5-fold for reactions 2−4 (Chart 1).

The kinetic parameters observed for the α,γ-elimination of MTA from (*S*,*S*)-SAM by E47Q and E47D ACC synthases substantiate the predicted role of Glu47 as an ionic complement to the positively charged sulfonium pole of SAM. It is a coincidence that the values of K_m for the WT and E47D reactions with (*S*,*S*)-SAM are identical, because the microscopic rate constants composing that parameter must be affected differentially by the mutations. The rate of the α,γ-elimination reaction catalyzed by WT enzyme is diffusion-controlled, but is not for E47D ACC synthase (see Figure 2). Therefore, for the WT enzyme, $K_m \gg K_d$, but K_m is a closer approximation to K_d for the mutant ACC synthases. The K_m value for E47D ACC synthase is only 5-fold lower than that characterizing the E47Q reaction, showing that side

[4] The large error in this measurement is probably due to an anomalous data point. The experiment was performed three times, twice yielding a partition ratio of <0.014 (i.e., no ACC was detected; the ratio was estimated on the basis of a lower limit for detection of ACC of 2 μM) and once yielding a partition ratio of 0.20.

Scheme 3: Possible Mechanisms for β,γ-Elimination of MTA from SAM[a]

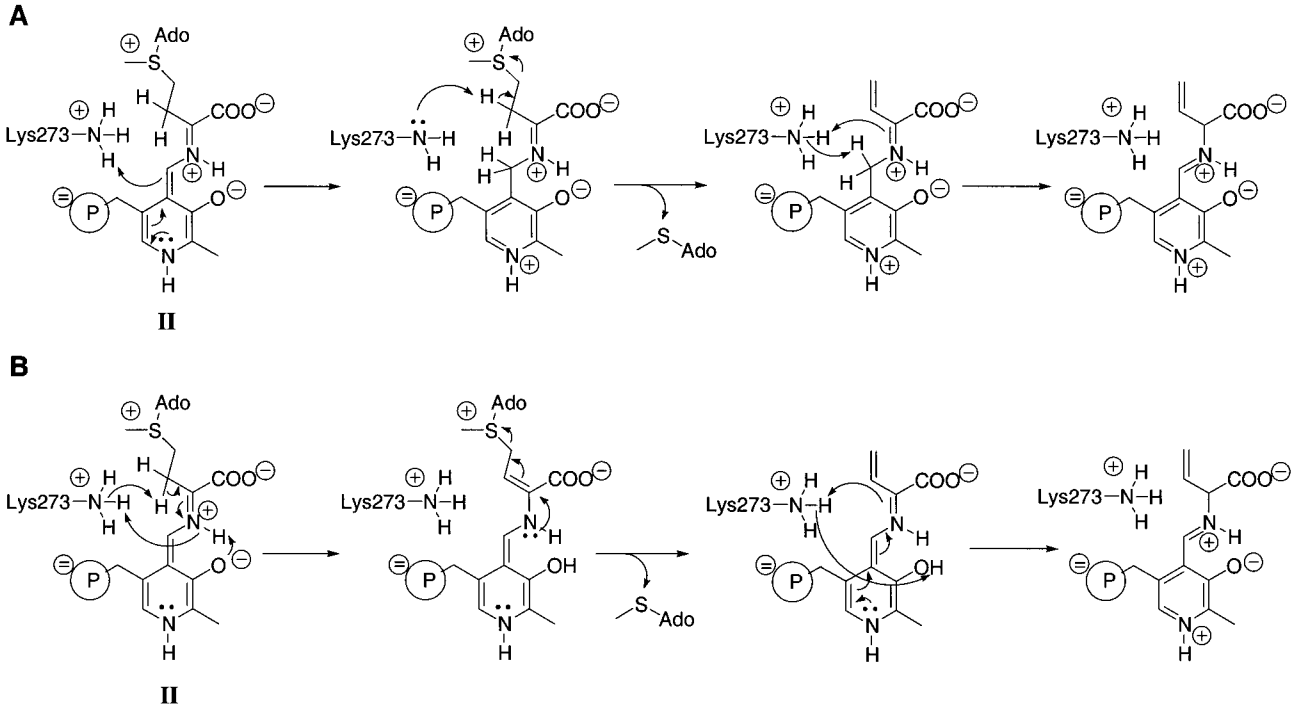

[a] (A) The SAM−PLP quinonoid intermediate (compound **II** from Scheme 1) is protonated at the C4′ position by Lys273, yielding a ketimine. Lys273 abstracts a C_β proton from the ketimine, initiating the β,γ-elimination of MTA, and the resulting ketimine is tautomerized to form the L-VG external aldimine. (B) The same products are formed without the transient ketimine intermediate.

chain charge, although suboptimally positioned, is more important than size.

The effects of the E47Q and E47D mutations of ACC synthase on the kinetic parameters for the β,γ-elimination of MTA from (*R*,*S*)-SAM are minor. The turnover numbers for each mutant decrease only 3-fold; the K_m value for E47Q increases 2-fold, while that of E47D remains unchanged relative to that of the WT enzyme. This small effect of the Glu47 mutations on binding of (*R*,*S*)-SAM at first seems contradictory to the proposed model of the active site interaction with the sulfonium ion. However, unfavorable steric hindrance associated with binding the (*R*,*S*) diastereomer of SAM probably overwhelms the favorable contribution of the ionic interaction between Glu47 and the sulfonium pole.

Kinetic parameters for deamination of L-VG and transamination of alanine by E47D and E47Q ACC synthase are also not significantly altered compared to those of the WT enzyme. The largest effect is that the E47Q mutation shows a 5-fold decrease in K_m for deamination of L-VG compared to that with WT. Apparently, the presence of the negative charge at Glu47 slightly decreases the affinity of ACC synthase for L-VG. The observation that binding of L-VG and alanine to ACC synthase is only moderately influenced by mutation of Glu47 is predicted by the ion pair interaction model, since the negative charge of Glu47 should not effect association of these neutral side chain substrates.

Possible Roles for Glu47 in Catalysis by ACC Synthase. The E47Q and E47D mutations of ACC synthase decrease k_{cat} for the α,γ-elimination of MTA from (*S*,*S*)-SAM by 110- and 5-fold, respectively. Since the microscopic rate constants that control k_{cat} are not influenced by whether association of the enzyme with substrate is rate-determining, Glu47 must make a contribution to catalysis as well as to substrate association.

The α,γ-elimination reaction (Scheme 1) consists of a sequence of five steps involving transaldimination with (*S*,*S*)-SAM followed by C_α-proton abstraction, elimination of MTA, transaldimination of the ACC external aldimine to release enzyme-bound ACC, and finally release of ACC from the enzyme. The rate of product release is not limiting for E47D ACC synthase, since k_{cat} for the α,γ-elimination reaction is insensitive to viscosity (L. Feng, unpublished results); therefore, Glu47 must have a specific influence on one or more of the chemical steps involved in the α,γ-elimination reaction.

Glu47 may directly influence the rate of the α,γ-elimination of MTA from (*S*,*S*)-SAM by ACC synthase by providing an anchor point for the sulfonium pole of SAM, thus positioning the substrate correctly for the ensuing chemistries. The short distance between the ϵ-nitrogen of Lys273 and the carboxylate oxygen of Glu47 in the model (3.1 Å) raises the additional possibility that Glu47 may function as a general base, assisting in the deprotonation of Lys273 prior to transaldimination of the ACC aldimine. To our knowledge, however, such an interaction between the catalytic lysine and an active site general base is unprecedented in PLP-dependent enzymes.

Glu47 Influences the ($\alpha,\gamma/\beta,\gamma$)-Elimination Ratio for (R,S)-SAM. The k_{cat} value for α,γ-elimination of MTA from (*R*,*S*)-SAM by WT ACC synthase is 0.031 s^{-1},[5] 580-fold lower than the k_{cat} for the same reaction with (*S*,*S*)-SAM. This decrease in k_{cat} is most likely due to the fact that the sulfonium methyl group of (*R*,*S*)-SAM shields the electrostatic interaction between the sulfonium pole and Glu47, thus

[5] The k_{cat} value for α,γ-elimination of MTA from (*R*,*S*)-SAM by WT ACC synthase was obtained by multiplying the k_{cat} value for β,γ-elimination of MTA from the same substrate (Table 1) by 0.4, the ($\alpha,\gamma/\beta,\gamma$)-elimination partition ratio for (*R*,*S*)-SAM.

interfering with establishment of the correct substrate orientation for α,γ-elimination. The pathways for α,γ- and β,γ-elimination of MTA from ACC synthase most likely diverge at the common quinonoid intermediate (Scheme 3). Formation of a cyclopropane ring distorts the normal carbon−carbon bond angles, and thus imposes severe geometric constraints on the transition state leading from the quinonoid to ACC. The topology of the active site that includes inter alia Glu47 serves to impose these constraints on the natural diastereomer, (*S*,*S*)-SAM. The interactions of (*R*,*S*)-SAM with Glu47 are different (as discussed above); thus, the more facile β,γ-elimination reaction predominates, yielding an (α,γ/β,γ)-elimination ratio of 0.4 for the WT enzyme. The decreases in the (*R*,*S*)-SAM (α,γ/β,γ)-elimination ratios of the E47Q and E47D enzymes relative to that of WT, together with the observation that these mutations have only small effects on the rates of β,γ-elimination, require that Glu47 participate in guiding even (*R*,*S*)-SAM to α,γ-elimination.

ACKNOWLEDGMENT

We thank Andrew C. Eliot and Dr. Keith A. Koch for stimulating discussions.

REFERENCES

1. Yang, S. F., and Hoffman, N. E. (1984) *Annu. Rev. Plant Physiol. 35*, 155−189.
2. White, M. F., Vasquez, J., Yang, S. F., and Kirsch, J. F. (1994)- *Proc. Natl. Acad. Sci. U.S.A. 91*, 12428−12432.
3. Li, Y., Feng, L., and Kirsch, J. F. (1997) *Biochemistry 36*, 15477−15488.
4. Ramalingam, K., Lee, K. M., Woodard, R. W., Bleecker, A. B., and Kende, H. (1985) *Proc. Natl. Acad. Sci. U.S.A. 82*, 7820−7824.
5. Adams, D. O., and Yang, S. F. (1979) *Proc. Natl. Acad. Sci. U.S.A. 76*, 170−174.
6. Satoh, S., and Yang, S. F. (1989) *Plant Physiol. 91*, 1036−1039.
7. Satoh, S., and Yang, S. F. (1989) *Arch. Biochem. Biophys. 271*, 107−112.
8. Feng, L., and Kirsch, J. F. (2000) *Biochemistry 39*, 2436−2444.
9. Feng, L., Geck, M. K., Eliot, A. C., and Kirsch, J. F. (2000) *Biochemistry 39*, 15242−15249.
10. Capitani, G., Hohenester, E., Feng, L., Storici, P., Kirsch, J. F., and Jansonius, J. N. (1999) *J. Mol. Biol. 294*, 745−756.
11. Kleywegt, G. J., and Jones, T. A. (1998) *Acta Crystallogr. D54*, 1119−1131.
12. Jones, T. A., and Kjeldgaard, M. (1991) *Manual for O (verseion 5.6)*, Uppsala University, Uppsala, Sweden.
13. Artamonova, E. Y., Zavalova, L. L., Khomutov, R. M., and Khomutov, A. R. (1986) *Bioorg. Khim. 12*, 206−212.
14. Park, J., Tai, J., Roessner, C. A., and Scott, A. I. (1996) *Bioorg. Med. Chem. 4*, 2179−2185.
15. Osaki, S., and Schowen, R. L. (1978) in *Nucleic Acid Chemistry* (Townsend, L. B., and Tipson, R. S., Eds.) p 889, Wiley, New York.
16. Stolowitz, M. L., and Minch, J. M. (1981) *J. Am. Chem. Soc. 103*, 6015−6019.
17. Hoffman, J. L. (1986) *Biochemistry 25*, 4444−4449.
18. Beaudouin, C., Haurat, G., Lafitte, J. A., and Renaud, B. (1993) *J. Neurochem. 61*, 928−935.
19. Fields, R. (1972) *Methods Enzymol. 25*, 464−478.
20. Li, R., and Kenyon, G. L. (1995) *Anal. Biochem. 230*, 37−40.
21. Brouwer, A. C., and Kirsch, J. F. (1982) *Biochemistry 21*, 1302−1307.
22. Blacklow, S. C., Raines, R. T., Lim, W. A., Zamore, P. D., and Knowles, J. R. (1988) *Biochemistry 27*, 1158−1167.
23. Dunford, H. B., and Hewson, W. D. (1977) *Biochemistry 16*, 2949.
24. Satoh, S., and Esashi, Y. (1986) *Plant Cell Physiol. 27*, 285−291.
25. Satoh, S., and Yang, S. F. (1988) *Plant Physiol. 88*, 109−114.
26. Khani-Oskouee, S., Jones, J. P., and Woodard, R. W. (1984) *Biochem. Biophys. Res. Commun. 121*, 181−187.
27. McPhalen, C. A., Vincent, M. G., Picot, D., Jansonius, J. N., Lesk, A. M., and Chothia, C. (1992) *J. Mol. Biol. 227*, 197−213.
28. Djordjevic, S., and Stock, A. M. (1997) *Structure 5*, 545−558.
29. Schluckebier, G., O'Gara, M. O., Saenger, W., and Cheng, X. (1995) *J. Mol. Biol. 247*, 16−20.
30. Fu, Z., Hu, Y., Konishi, K., Takata, Y., Ogawa, H., Gomi, T., Fujioka, M., and Takusagawa, F. (1996) *Biochemistry 35*, 11985−11993.
31. Ekstrom, J. L., Mathews, I. I., Stanley, B. A., Pegg, A. E., and Ealick, S. E. (1999) *Structure 7*, 583−595.
32. Kraulis, P. J. (1991) *J. Appl. Crystallogr. 24*, 946−950.

BI011050Z